

Simulation of a Hybrid Concentrated Solar and Biomass-Fuelled Trigeneration System for Residential Applications

Luca Cioccolanti^{1,*} , Greta Lombardi¹ , Luca Del Zotto¹ , and Pietro Elia Campana² 

¹Research Centre for Energy, Environment and Landscape (CREAT), Italy

²Mälardalen University, Sweden

*Correspondence: Luca Cioccolanti, luca.cioccolanti@uniecampus.it

Abstract. Solar technologies stand out as effective solutions for decarbonising the building sector. Among them, Concentrated Solar Power (CSP) systems offer the advantage of delivering flexible and dispatchable power. However, hybridisation with other renewable energy sources is often pursued to extend the operational hours. Therefore, this study investigates the complementarity of solar energy with biomass combustion within a small-scale hybrid tri-generative plant. More precisely, the proposed system consists of a 240 kW_{th} peak thermal power Linear Fresnel Reflectors solar field combined with a 130 kW_{th} back-up biomass boiler to supply heat to a 20 kW_{el}/100 kW_{th} Organic Rankine Cycle (ORC) unit for the provision of cooling, heating and electric power to 10 apartments. The hybrid plant also integrates thermal energy storage tanks and a battery energy system to increase the solar energy self-consumption and reduce the intervention of the grid. The performance of the hybrid system is analysed through an advanced simulator developed by the authors in MATLAB/Simulink considering the components' inertia. The results reveal an increment in solar energy self-consumption achieved by exploiting the low solar irradiance to bring the latent heat thermal energy storage into its melting range, thereby extending ORC operation into nighttime hours. More precisely, the system meets the entire annual thermal demand for space heating, cooling and domestic hot water through renewable sources, consuming 2.25 tons of biomass. Electric demand coverage, instead, reaches up to 81% with the inclusion of a 60 kWh_{el} battery energy storage system.

Keywords: Renewable Energy Sources Complementarity, Concentrated Solar Power, Hybrid CSP-Biomass System, Organic Rankine Cycle, Combined Cooling Heating and Power

1. Introduction

According to IRENA, the global cumulative installed renewable electricity capacity needs to triple from 2022 to 2030 reaching more than 11'000 GW to limit the surface temperature increase to 1.5°C above pre-industrial levels [1]. This capacity addition would be dominated by variable Renewable Energy Technologies (vRETs), such as photovoltaics (PV) and wind turbines, bringing pressure to grid stability as it is not designed to deal with the fluctuating nature of intermittent renewable sources.

Compared to other solar energy technologies, concentrated solar power (CSP) can deliver flexible and dispatchable power thus allowing the allocation of a large capacity of vRETs.

Therefore, despite being less economically appealing than other RETs, CSP systems have recently attracted attention with special interest in their hybridisation with other vRETs.

In the literature, hybrid plants combining CSP with wind, PV, and biomass systems have been largely investigated at medium to large scales. For example, Liu et al. [2] conducted a techno-economic analysis of a PV and CSP system integrated by electrical and thermal storage systems under a constant 100 MW load demand. Similarly, Petrollese et al. [3] focused on the optimal design parameters of a combined CSP, PV and battery system to minimise energy production costs for a constant power output of 1 MW. Liu et al. [4], instead, analysed twelve locations in China with two distinct load demand profiles to minimise the levelized cost of energy (LCOE) including and optimising the size of PV, wind turbines, batteries, hydrogen storage, thermal energy storage and CSP technologies. Results have shown that thermal storage with batteries was more effective than hydrogen storage with batteries. Similarly, an evaluation of the LCOE of two 1 MW hybrid CSP/biomass power plants installed in Tunis, one for power generation and the other for combined heat and power (CHP) production, has been conducted by Soares et al. [5]. They reported a lower cost of energy in CHP configuration with a value of 126.3 €/MWh_{el} compared to 175.4 €/MWh_{el} in power configuration only.

Contrarily, due to their reduced competitiveness, few works on hybrid CSP systems at small scales are available in the literature. Costa et al. [6] performed an environmental and economic analysis of an innovative CSP-PV system using a beam splitter for more efficient use of solar irradiance for two locations in Europe. In a previous work [7], some of the authors of the present study have investigated hybrid CSP-wind trigenerative systems for the provision of cooling, heating and electrical power for residential applications, finding an improved renewable energy self-consumption and reduced grid reliance. Also in the case of hybrid CSP+PV integrated with power-to-grid electric vehicles [8] the performance of hybrid CSP with vRETs resulted in limited energy production compared to user demand.

The literature review carried out has revealed that small-scale hybrid power plants based on CSP technologies have been marginally investigated, and this work aims at filling the gap by considering the hybridisation of a micro-scale CSP system with a biomass pellet boiler for the full provision of user thermal energy demand by renewables.

2. Methods and models

The hybrid system under investigation combines solar and biomass energy sources to supply heat to an organic Rankine cycle (ORC) unit for the provision of cooling, heating, and electric power to 10 apartments located in central Italy. As depicted in Figure 1, the system comprises the following key components:

- a 440 m² linear Fresnel reflectors (LFR) solar field, having a peak thermal power of approximately 240 kW_{th} generating heat in the temperature range of 280°C - 320°C;
- a 130 kW_{th} biomass-fired boiler (BFB) using wood chips as fuel;
- a 20 kW_{el}/100 kW_{th} regenerative ORC system, utilising toluene as working fluid;
- a 19 tons NaNO₂(6wt.%) / NaNO₃(94wt.%) latent heat thermal energy storage (LHTES) system, able to ensure 6 hours of ORC operation without sunlight by storing about 800 kWh_{th} of thermal energy from the solar field;
- a 7 m³ sensible heat thermal energy storage (SHTES), acting as a buffer between the ORC unit and the users;
- an 80 kW_c single-stage cooling absorption chiller (ABS) using a lithium bromide-water solution for space cooling during summer;
- a dry cooler to dissipate excess heat from the ORC unit condenser;
- a 60 kW_{el} lithium-ion battery energy storage system (BESS), to reduce the power exchange with the external grid and increase solar energy self-consumption.

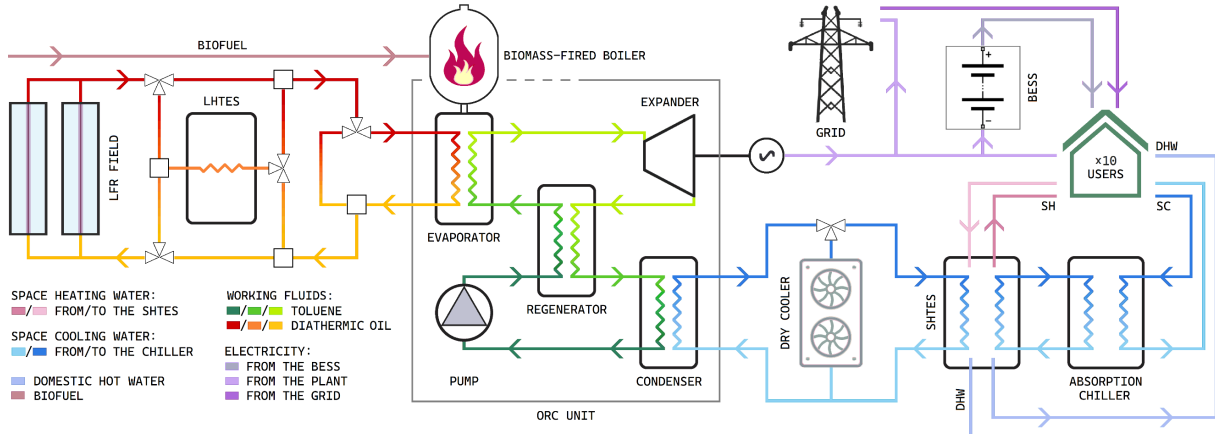


Figure 1. Diagram of the hybrid solar plant

The hybrid plant works under various operating modes (OMs) devised to use solar and biomass sources in series to run the ORC. The plant's controls aim at satisfying the entire thermal load, while electricity production is stored in the BESS or exchanged with the grid in case of mismatches with user demands. Table 1 lists the possible OMs and the related operating conditions:

Table 1. Operating conditions of the CSP system for each OM

OM	Sub-systems	Operating Conditions
-4	BFB + ORC	<i>if</i> $OM = 0 \parallel OM = -1 \parallel OM = +1$ & $P_{el,demand} > P_{el,ORC,min}$ <i>then</i> $0.05 \text{ kg/s} < \dot{m}_{fuel} < 0.10 \text{ kg/s}$
-3	LFR + LHTES + ORC	<i>if</i> $P_{th,LFR,out} < 65 \text{ kW}_{th}$ & $T_{LHTES} > T_{ORC,off}$ <i>then</i> $\dot{m}_{oil} = 3.0 \text{ kg/s}$
-2	LFR recirculation	<i>if</i> $P_{th,LFR,out} < 65 \text{ kW}_{th}$ & $T_{LFR,out} < T_{LHTES} + 10^\circ\text{C}$ <i>then</i> $\dot{m}_{oil} = 1.0 \text{ kg/s}$
-1	LHTES + ORC	<i>if</i> $P_{th,LFR,out} = 0 \text{ kW}_{th}$ & $T_{LHTES} > T_{ORC,off}$ <i>then</i> $\dot{m}_{oil} = 2.0 \text{ kg/s}$
0	OFF state	<i>if</i> $P_{th,LFR,out} = 0 \text{ kW}_{th}$ & $P_{el,demand} < P_{el,ORC,min}$ <i>then</i> $\dot{m}_{oil} = 0.0 \text{ kg/s}$
1	LFR + LHTES	<i>if</i> $P_{th,LFR,out} < 65 \text{ kW}_{th}$ & $T_{LFR,out} > T_{LHTES} + 10^\circ\text{C}$ <i>then</i> $\dot{m}_{oil} = 3.0 \text{ kg/s}$
2	LFR + ORC	<i>if</i> $65 \text{ kW}_{th} < P_{th,LFR,out} < 130 \text{ kW}_{th}$ <i>then</i> $1.0 \text{ kg/s} < \dot{m}_{oil} < 2.0 \text{ kg/s}$
3	LFR + LHTES + ORC	<i>if</i> $P_{th,LFR,out} > 130 \text{ kW}_{th}$ & $T_{LHTES} < 320^\circ\text{C}$ <i>then</i> $2.5 \text{ kg/s} < \dot{m}_{oil} < 5.0 \text{ kg/s}$, else OM 4
4	LFR (defocus) + ORC	<i>if</i> $305^\circ\text{C} < T_{LHTES} < 310^\circ\text{C}$ with hysteresis <i>then</i> $\dot{m}_{oil} = 2.0 \text{ kg/s}$

The model is developed in MATLAB/Simulink [9] while user demand for space heating and cooling is obtained from TRNSYS [10]. Hot water demand is calculated according to the European standard UNI EN15316-3, whereas electricity consumption - which excludes space heating and cooling loads, is assessed with a time step of 10 minutes as in reference [7]. Dynamic models represent the plant's components, except for the ORC unit, the dry cooler, and the absorption chiller, due to their significantly lower thermal inertia compared to the TES and piping systems.

2.1 Modelling of the main components

The performance of the LFR solar field is evaluated in terms of its optical efficiency, η_{opt} , and receiver efficiency, η_{rec} , as follows:

$$\eta_{opt} = \eta_{opt,max}(\theta = 0) \cdot IAM(\alpha, \sigma) \quad (1)$$

where $\eta_{opt,max}$ is the maximum optical efficiency, achieved when the incident angle θ equals zero, and IAM is the Incident Angle Modifier, provided by a manufacturing company for a downscaled system. The receiver efficiency, instead, is calculated through an improved one-dimensional Forristall model as detailed in a previous work by some of the authors [11]. Therefore, the thermal power output from the solar field $P_{LFR,out}$ amounts to:

$$P_{LFR,out} = A_{sf} \cdot DNI \cdot \cos(\theta) \cdot \eta_{opt} \cdot \eta_{rec} \quad (2)$$

where A_{sf} is the area of the solar field and DNI is the Direct Normal Irradiance.

The biomass furnace is modelled assuming complete combustion with 20% air excess and wood chip properties provided by [12]. The furnace's dynamic behaviour is simulated by applying the transfer function formulated in [12] to the following energy balance equation:

$$\dot{m}_f \cdot NCV + \dot{m}_f \cdot h_f(T_f) + \dot{m}_a \cdot h_a(T_a) = \dot{m}_g \cdot h_g(T_g) + \dot{Q}_{loss} \quad (3)$$

where \dot{m}_a , \dot{m}_f , \dot{m}_g , h_a , h_f , h_g are respectively the mass flow rate and the specific enthalpy of the inlet air, biofuel and exhaust gases, \dot{Q}_{loss} the heat losses by radiation, and NCV the net calorific value calculated considering the fuel's moisture and hydrogen content.

The performance of the ORC unit is evaluated in terms of electrical and thermal power output by iteratively solving the system based on the changing operating conditions:

$$P_{ORC,el} = \dot{m}_f \cdot [\eta_m \cdot \eta_{el} \cdot \Delta h_e - \Delta h_p / (\eta_m \cdot \eta_{el})] \quad (4)$$

$$P_{ORC,th,out} = \dot{m}_c \cdot c_{p,c} \cdot (T_{out,c} - T_{in,c}) \quad (5)$$

where \dot{m}_f is the organic fluid mass flow rate, η_m and η_e the mechanical and electrical efficiencies, Δh_e and Δh_p the enthalpy difference at the expander and pump respectively, while \dot{m}_c , $c_{p,c}$, $T_{out,c}$ and $T_{in,c}$ are the cooling water's mass flow rate, specific heat, outlet and inlet temperatures at the condenser.

Both the LHTES and the SHTES are simulated using a dynamic model due to their high thermal inertia having a relevant impact on the performance of the entire plant. The temperature variation and heat exchanged by the phase-change material (PCM) of the LHTES are calculated based on the IEA Task32 guidelines [13], while for the SHTES the following energy balance is calculated:

$$m_w c_{p,w} \frac{dT_{SHTES}}{dt} = P_{th,coil} - P_{th,DHW} - P_{th,SH} - P_{th,ABS,in} - P_{th,SHTES,loss} \quad (6)$$

where m_w and $c_{p,w}$ are the mass and specific heat of the water inside the SHTES, while $P_{th,coil}$, $P_{th,DHW}$, $P_{th,SH}$, $P_{th,ABS,in}$ and $P_{th,SHTES,loss}$ are the thermal power exchanged by the coil, required for domestic hot water, space heating, by the absorption chiller, and losses of the SHTES, respectively.

2.2 Modelling of the balance of the plant and the control logic

The pipes are modelled using a one-dimensional longitudinal advection equation, and the performance of the absorption chiller is represented by a polynomial curve derived from the data reported by the manufacturer [14]. Hot water from the SHTES provides heat to the generator, and - known the cooling demand required by the users and the COP of the absorption chiller for given operating conditions, the thermal power required by the absorption chiller is calculated and then subtracted from the energy content of the water in the SHTES according to equation 6.

The control logic of the plant has been conceived to limit biomass consumption while ensuring the full provision of thermal demands. Hence, the ORC system operates at part-load conditions powered by the biomass boiler or the solar field whenever the condenser's thermal production surpasses the thermal demand, or at full load to meet the peaks in electricity requirements.

3. Results

Simulations are performed for a solar year with a time step of 1 minute considering the plant installed in Ancona, a seaside mid-town in central Italy. Figure 2 and 3 illustrate the trends for a typical winter and summer day respectively.

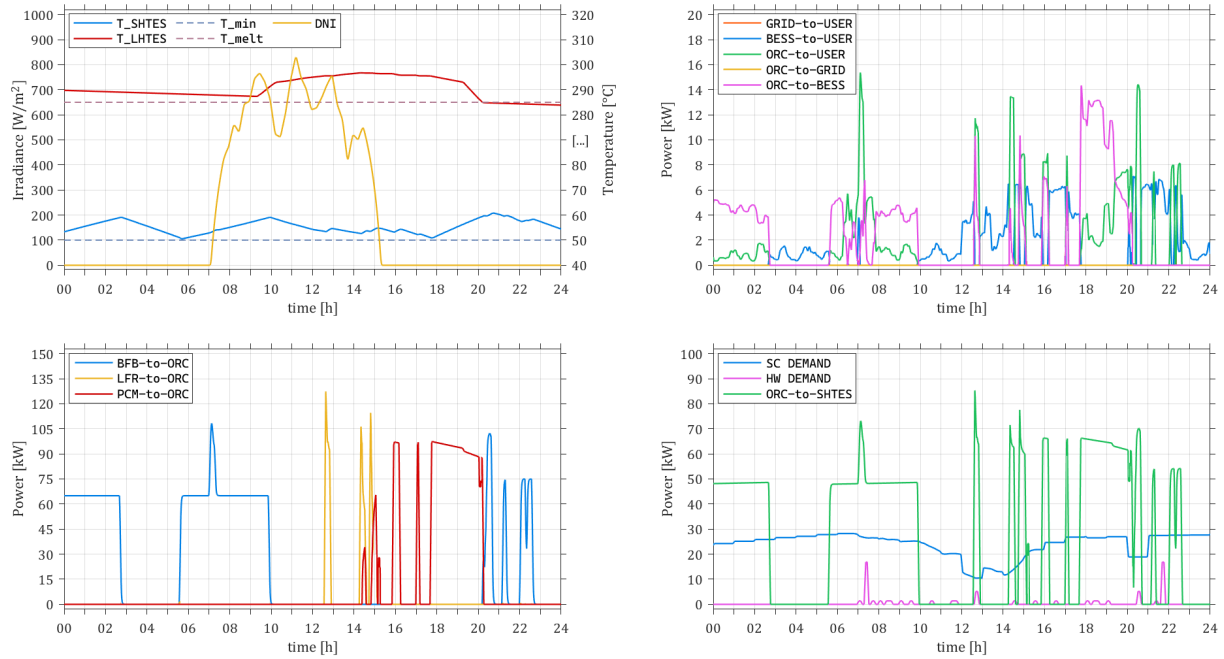


Figure 2. Power exchange and temperature trends of system components on a typical winter day

As can be noticed in Figure 2, during the early morning of a winter day, the ORC operates fuelled by the biomass boiler generating electricity surplus which the BESS stores. The LHTES records a temperature around the melting point throughout the first half of the day, therefore, the biomass boiler engages twice to maintain the tank's water temperature for space heating (SH) and domestic hot water (HW) requirements, and once for the coverage of electric demands. Meanwhile, the LFR recirculates to raise the PCM's temperature, ultimately enabling the storage's utilisation to cover the evening's peaks. Conversely, during the summer day depicted in Figure 3, the higher availability of solar power obviates the need for boiler activations. The LHTES temperature remains above the melting point throughout the day, leveraging the afternoon's peak sunlight hours to store excess heat collected by the LFRs, while the ORC operates nearly uninterruptedly.

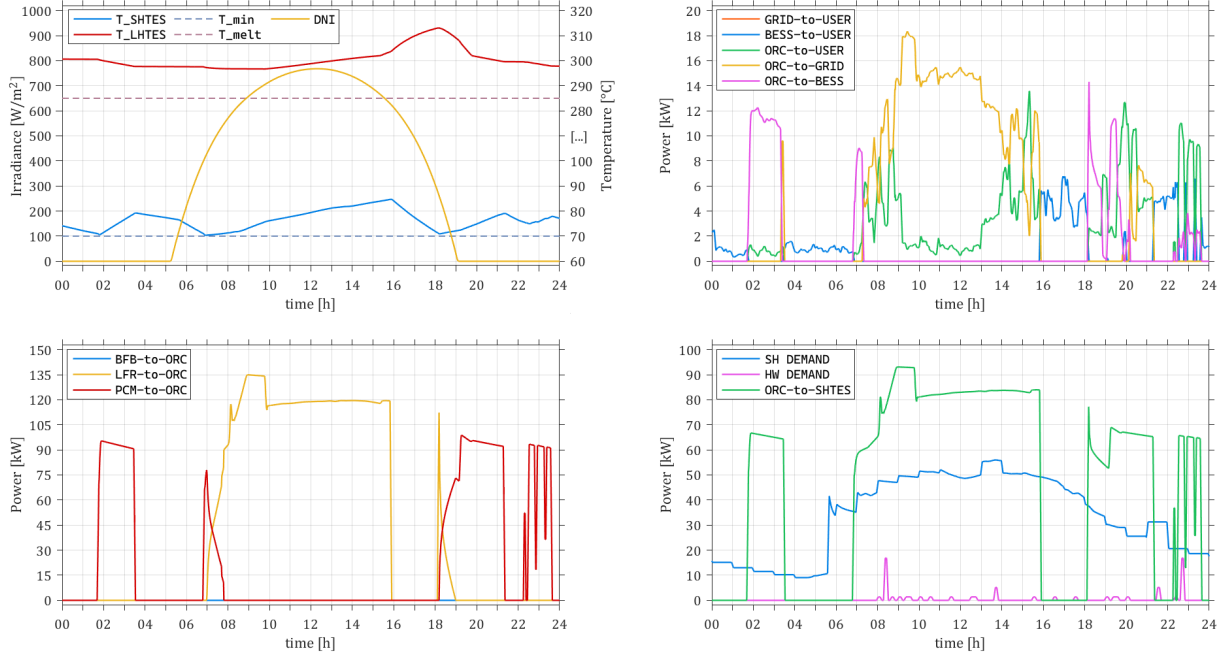


Figure 3. Power exchange and temperature trends of system components on a typical summer day

Figure 4 and Figure 5 depict the plant's electrical and thermal energy supply on a monthly basis. As anticipated by the daily trends, the contribution of biomass combustion peaks in wintertime while dropping below 5% in summer. Independently from the source employed, the ORC is responsible for supplying between 35% and 70% of electricity demands, thus not sufficing the entire load despite producing nearly double the amount in excess. This behaviour is justified by the control logic imposing the operation of the unit to maintain the SHTES within a desirable temperature range regardless of the current electrical demand, in order to maximise solar energy self-consumption for space heating, cooling and domestic hot water.

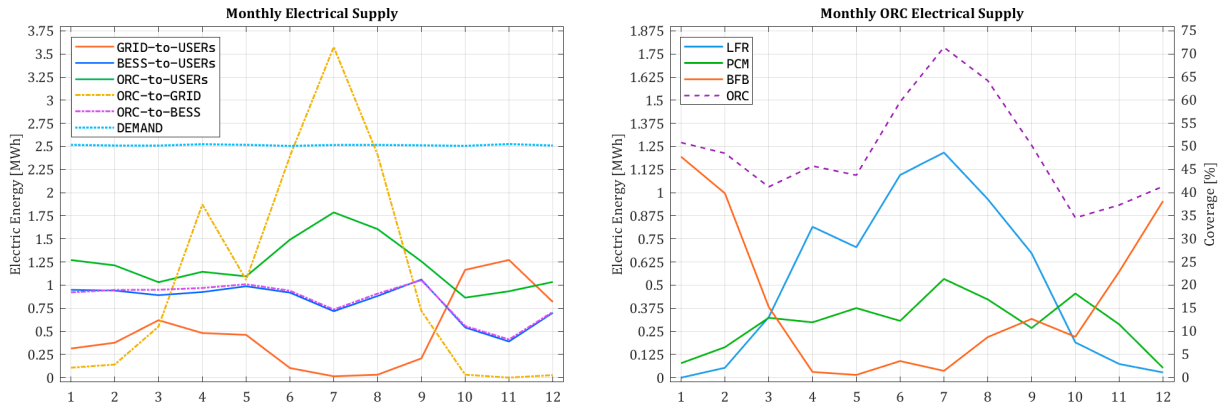


Figure 4. Monthly electric energy supply

Additionally, the figures detail the components' contributions to the ORC electrical and thermal production. The unit's utilisation of heat from the LHTES appears negligible during the coldest months, however, it is noteworthy that the PCM's contribution surpasses that of the heat directly received from the solar field, proving the hybrid plant capable of enhancing system flexibility for load-shifting. Furthermore, the boiler's inactivity during summer increases the holistic value of hybridisation.

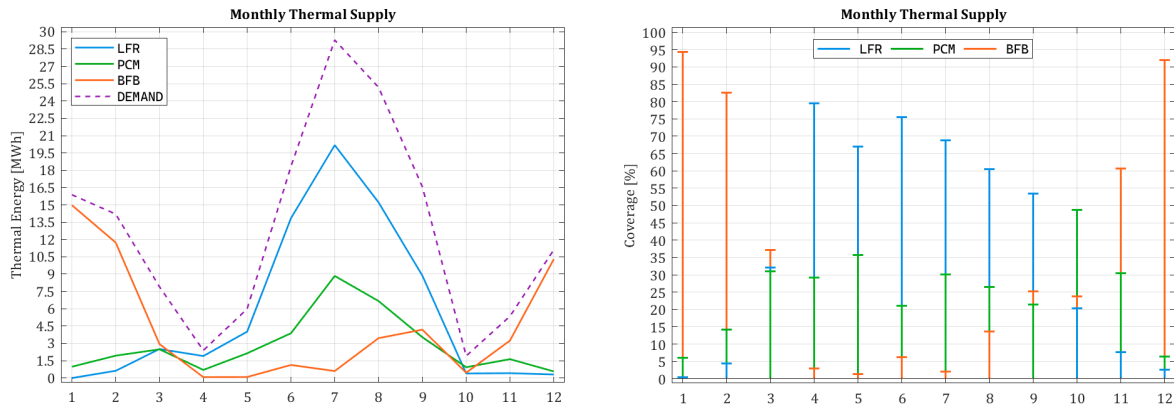


Figure 5. Monthly thermal energy supply

Considering the entire year, the CSP system supplies 66.5% of thermal demands, while the boiler provides the remaining 34.5%. As a consequence, the annual biomass consumption amounts to 2.25 tons, largely attributed to winter's space heating requirements.

4. Conclusions

The performed analysis shows the suitability of hybridising a CSP-ORC system with a biomass pellet boiler for the provision of cooling, heating and power to 10 apartments in a location in central Italy. The proposed hybrid system configuration makes possible to increase solar energy self-consumption by increasing the LHTES role during the cold season compared to the CSP system alone.

During summertime, the solar energy collected by the CSP is able to provide the required input to the ORC unit to almost fully satisfy the cooling demand, greatly limiting the operation of the biomass-fired boiler.

Compared to previous studies performed by some of the authors, which considered CSP-wind and CSP-PV hybridizations, the present configuration is able to fully satisfy thermal energy demands by renewables with a significant reduction in CO₂ emissions. Nevertheless, it still results in a significant electricity excess sold to the grid, which could be reduced by more advanced control logic as the scope of future works.

Data availability statement

Data will be made available on request.

Author contributions

Luca Cioccolanti: Writing – review & editing, Supervision, Methodology, Validation, Data curation, Greta Lombardi: Writing – original draft, Validation, Software, Methodology, Investigation, Formal analysis. Luca Del Zotto: Writing – review & editing, Supervision, Pietro Elia Campana: Writing – review & editing, Visualization, Methodology.

Competing interests

The authors declare that they have no competing interests.

Funding

No external funding has been received.

References

- [1] "Tripling renewable power and doubling energy efficiency by 2030: Crucial steps towards 1.5°C." Accessed: Sep. 26, 2024. [Online]. Available: <https://www.irena.org/Digital-Report/Tripling-renewable-power-and-doubling-energy-efficiency-by-2030#page-1>
- [2] T. Liu, J. Yang, Z. Yang, and Y. Duan, "Techno-economic feasibility of solar power plants considering PV/CSP with electrical/thermal energy storage system," *Energy Convers Manag*, vol. 255, p. 115308, Mar. 2022, doi: [10.1016/j.enconman.2022.115308](https://doi.org/10.1016/j.enconman.2022.115308).
- [3] M. Petrollese and D. Cocco, "Optimal design of a hybrid CSP-PV plant for achieving the full dispatchability of solar energy power plants," *Solar Energy*, vol. 137, pp. 477–489, 2016, doi: [10.1016/j.solener.2016.08.027](https://doi.org/10.1016/j.solener.2016.08.027).
- [4] T. Liu, J. Li, Z. Yang, and Y. Duan, "Evaluation of the short- and long-duration energy storage requirements in solar-wind hybrid systems," *Energy Convers Manag*, vol. 314, p. 118635, Aug. 2024, doi: [10.1016/j.enconman.2024.118635](https://doi.org/10.1016/j.enconman.2024.118635).
- [5] J. Soares, A. C. Oliveira, S. Dieckmann, D. Krüger, and F. Orioli, "Evaluation of the performance of hybrid CSP/biomass power plants," *International Journal of Low-Carbon Technologies*, vol. 13, no. 4, pp. 380–387, Dec. 2018, doi: [10.1093/ijlct/cty046](https://doi.org/10.1093/ijlct/cty046).
- [6] D. Costa et al., "Environmental and economic impacts of photovoltaic integration in concentrated solar power plants," *Solar Energy*, vol. 274, p. 112550, May 2024, doi: [10.1016/j.solener.2024.112550](https://doi.org/10.1016/j.solener.2024.112550).
- [7] L. Cioccolanti, R. Tascioni, R. Moradi, and J. Jurasz, "Investigating the hybridisation of micro-scale concentrated solar trigeneration systems and wind turbines for residential applications using a dynamic model," *Energy Convers Manag*, vol. 269, p. 116159, Oct. 2022, doi: [10.1016/j.enconman.2022.116159](https://doi.org/10.1016/j.enconman.2022.116159).
- [8] G. Lombardi, L. Cioccolanti, L. Del Zotto, S. Tomassetti, and P. E. Campana, "The role of electric vehicles in hybrid solar-based small energy communities," *Energy Convers Manag*, vol. 321, p. 119074, Dec. 2024, doi: [10.1016/j.enconman.2024.119074](https://doi.org/10.1016/j.enconman.2024.119074).
- [9] Simulink, "Simulink - Simulation and Model-Based Design - MATLAB & Simulink," Simulation and Model-Based Design. Accessed: May 02, 2024. [Online]. Available: <https://www.mathworks.com/products/simulink.html>
- [10] "TRNSYS : Transient System Simulation Tool." Accessed: May 02, 2024. [Online]. Available: <http://www.trnsys.com/>
- [11] R. Tascioni, L. Cioccolanti, P. Pili, and E. Habib, "Preliminary estimation of the receiver tube wall temperature and the performance of CSP plants in off design-conditions by means of a simplified dynamic model," *Energy Convers Manag*, vol. 257, p. 115379, Apr. 2022, doi: [10.1016/j.enconman.2022.115379](https://doi.org/10.1016/j.enconman.2022.115379).
- [12] M. Pirouti, J. Wu, J. B. Ekanayake, and N. Jenkins, "Dynamic modelling and control of a direct-combustion biomass CHP unit," in 45th International Universities Power Engineering Conference UPEC2010, Cardiff, UK, 2010.
- [13] P. Gantenbein, D. Jaenig, H. Kerskes, and M. Van Essen, "Final report of Subtask B; Chemical and Sorption Storage; The overview A Report of IEA Solar Heating and Cooling programme -Task 32 Advanced storage concepts for solar and low energy buildings Report B7 of Subtask B," 2008, Accessed: May 02, 2024. [Online]. Available: <http://task32.iea-shc.org/data/sites/1/publications/task32-b7.pdf>
- [14] "Yazaki Energy Systems, Inc." Accessed: May 02, 2024. [Online]. Available: <http://www.yazakienergy.com/waterfiredperformance.html>